

# Inflations prior to Vulcanian eruptions and gas bursts detected by tilt observations at Semeru Volcano, Indonesia

Takeshi Nishimura · Masato Iguchi ·  
Ryohei Kawaguchi · Surono · Muhamad Hendrasto ·  
Umar Rosadi

Received: 29 May 2011 / Accepted: 30 November 2011 / Published online: 14 February 2012  
© Springer-Verlag 2012

**Abstract** We examine the basic characteristics of inflations at Semeru Volcano, Indonesia, to clarify the pressurization process prior to two different styles of explosive eruptions: Vulcanian eruptions and gas bursts. Analysis of data obtained from tilt meters installed close to the active crater allows clarification of the common features and the differences between the two styles of eruptions. To improve the signal-to-noise ratio and to determine the mean characteristics of the inflations, we stack tilt signals obtained from eruptions of different magnitudes and evaluate the maximum amplitude of the seismic signal associated with these eruptions. Vulcanian eruptions, which explosively release large amounts of ash, are preceded by accelerating inflation about 200–300 s before the eruption, which suggests volume expansion of the gas phase. In contrast, gas bursts, which rapidly effuse water steam accompanied by explosive sounds, follow non-accelerating changes of inflation starting 20 s before each emission. Tilt amplitudes increase with the magnitude of eruptions for both eruption styles. This suggests that the volume and/or pressure of magma or gas stored in the conduit before eruptions controls the magnitude of volcanic

eruptions. These results further suggest that the magnitude of eruptions can be predicted from geodetic measurements of volcano inflation.

**Keywords** Inflation · Tilt · Vulcanian eruption · Gas burst · Semeru · Prediction

## Introduction

Volcanoes display various styles of eruption during a sequence of eruptive activity. The magnitude and power of these eruptions also vary widely. The volatile behavior during the ascent of magma as it nears the surface plays an important role in the observed complexity of volcanic eruptions. Hence, it is important to have an understanding of gas behavior in order to clarify the mechanisms of magma ascent processes and eruptions and to predict eruption styles and magnitude in active volcanoes.

Recent studies based on geodetic observations have examined magmatic processes that precede various types of volcanic eruptions and magma ascent. For example, cyclic behavior identified in tilt records at Soufriere Hills, Montserrat Volcano (Voight et al. 1999), is a reflection of the nonlinear behavior of conduit flow, including microscale phenomena such as crystallization, gas loss by permeable flow, and viscosity increase due to degassing in magma (e.g., Melnik and Sparks 1999; Wylie et al. 1999). Detailed spatiotemporal dike distributions determined by GPS and tilt and strain data interpreted from magma ascent models with and without gas bubble growth are needed to understand the failed eruption of Mt. Iwate, Japan, in 1998 (Nishimura and Ueki 2011). Spatial changes of the strain data associated with an explosion in March 2004 at Soufriere Hills, Montserrat Volcano, are different from those observed in conjunction with the massive lava dome collapse

---

Editorial responsibility: M. Manga

---

T. Nishimura (✉) · R. Kawaguchi  
Department of Geophysics, Graduate School of Science,  
Tohoku University,  
Sendai 980-8578, Japan  
e-mail: nishi@zisin.gp.tohoku.ac.jp

M. Iguchi  
Sakurajima Volcano Research Center,  
Disaster Prevention Research Institute, Kyoto University,  
Kagoshima 891-1419, Japan

Surono · M. Hendrasto · U. Rosadi  
Center for Volcanology and Geological Hazard Mitigation,  
Bandung 40122, Indonesia

in July 2003, which suggests the presence of different magma systems beneath the volcano (Linde et al. 2009).

Recently, ground deformation measurements have also been conducted at sites close to the active crater during small Vulcanian or Strombolian eruptions. Active volcanoes with repeated eruptions are the best targets for geophysical measurements as much data can be acquired within a relatively short observation period. Several previous studies have addressed the magma processes associated with these eruptions based on deformation data as well as seismic, infrasonic, and other field data. Iguchi et al. (2008) examined deformation data at Sakurajima, Suwanosejima, and Semeru volcanoes and observed small-scale depressurization that occurs prior to explosions. They suggest that the depressurization triggers a rapid expansion of volatiles at great depths and that the duration of depressurization is related to the depth of the magma that expands rapidly to produce an eruption. Genco and Ripepe (2010) analyzed tilt data associated with more than 2,000 explosions at Stromboli Volcano. They showed that the volcano starts an inflation phase about 200 s before each explosion and that the inflation is temporally accelerated, which suggests gas bubble growth in the magma.

In the present study, we analyze tilt data recorded at Semeru Volcano in order to clarify the magmatic processes in the conduit. Semeru Volcano is well known for its frequent Vulcanian eruptions over the past few decades. However, following a period of dormancy from March to August 9, 2009, a lava dome appeared in November 2009, and the volcano exhibited gas bursts, which rapidly effused steam with explosive sounds. This change in the eruption style of the volcano allows a comparison of tilt data for Vulcanian eruptions with those for gas bursts. In the present paper, we clarify the basic characteristics of volcano inflation prior to eruptions of each type and discuss the differences in the process of magma ascent in the conduit before eruption.

### Volcanic activity of Semeru

Semeru volcano (8.108° S, 112.92° E; altitude, 3,676 m), located in East Java, Indonesia, is well known for its high volcanic activity. The volcano has had repeated Vulcanian eruptions with short repose times for many decades. These eruptions have produced a large amount of ash from the active crater named Jonggring Seloko. Each eruption produces volcanic plumes rising a few hundred up to a few thousand meters (Nishi et al. 2007; Iguchi et al. 2008) with significant variation in the magnitude of the eruptions. This eruptive activity, however, stopped suddenly in March 2009, and no subsequent surface activity was observed for 5 months. In August, volcanic earthquake activity restarted, and a new lava dome was observed in the active crater in

November of the same year. After that observation, lava collapses on the southeast flank have intermittently been observed from the Gunung Sawur Volcano Observatory (GSVO) located about 12 km east of the Semeru summit. Gas bursts started in January 2010. Only white clouds were produced by these emissions, suggesting that the exhalations were dominated by water steam. Visual observation conducted 500 m from the vent at the summit confirmed the absence of ash and pyroclastic materials in these emissions. Gas bursts occurred repeatedly at intervals ranging from a few minutes to tens of minutes and were accompanied by explosive sounds that were clearly heard at the summit. During the gas burst activity, lava collapses were sometimes observed on the southeast flank, suggesting that a new supply of magma was formed below. These observations, as well as the high altitude (about 3,500 m) of the active crater, suggest that this gas is not the result of interactions between magma and groundwater, but is probably derived from the separation of water vapor from magma in the conduit. These eruptive activities are illustrated in a series of photographs shown in Fig. 1.

### Tilt and seismic observations

Figure 2 shows the locations of tilt meters and seismometers used to record the data we analyzed in the present study. A temporary station was set at the summit (MHM) about 500 m north of the active crater. Data were collected at this station in March and April 2007, when Vulcanian eruptions occurred repeatedly; the station was equipped with a tilt meter (701-2, Applied Geomechanics) buried at a depth of 1 m and a STS-2 broadband seismometer (Streckeisen Ltd.). The tilt component radial to the active crater and the three-component velocity output of the STS-2 seismometer were digitized using a data logger LS7000-XT (Hakusan Co.) with 24-bit A/D resolution. The sampling frequencies were 1 and 100 Hz, respectively, for the tilt and seismic signals. We used data recorded from March 19 to April 11, 2007 for analysis.

In March 2010, when frequent gas bursts occurred, a tilt meter (Pinnacle Ltd., hybrid type, 1 nrad resolution, 1 Hz sampling) was again set at this station. From March 15 to April 2, 2010, two-component (NS and EW) tilt signals were digitized and saved in the internal memory of the tilt meter, and the data were uploaded every 6 h to an external data logger equipped with a GPS time correction function. We also set a short-period vertical component seismometer at the same location, and seismic signals from this station were telemetered via FM radio to GSVO. These signals were also digitized with a sampling frequency of 100 Hz and recorded by a data logger (LS7000) along with the signals from three seismic stations on the volcano flank (stations LEK, BSK, and TRT in Fig. 2). These stations

**Fig. 1** Photographs of volcanic activity of Semeru in 2009 and 2010. **a** Typical Vulcanian eruption at Semeru Volcano. **b** Close-up view of Vulcanian eruption. **c** Large Vulcanian eruption on November 15, 2007. **d** Lava dome in the crater in November 2009. **e** Gas burst at night in January 2010. **f** Night view of lava collapse on the southern flank in February 2010. **g** Gas burst at the summit crater. **h** White steam above the summit a few minutes after the gas burst shown in (g)

(a) Vulcanian eruption in 2007



(b) Vulcanian eruption seen from summit



(c) Large vulcanian eruption in 2007



(d) Lava dome (Nov. 5, 2009)



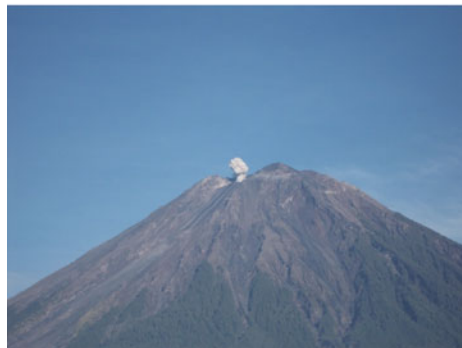
(e) Gas burst at night (Jan. 7, 2010)



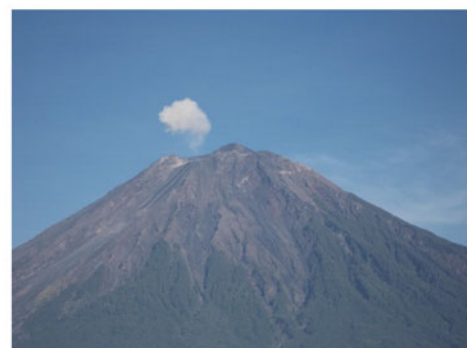
(f) Lava flow (Feb. 26, 2010)



(g) Gas burst (Mar. 11, 2010)



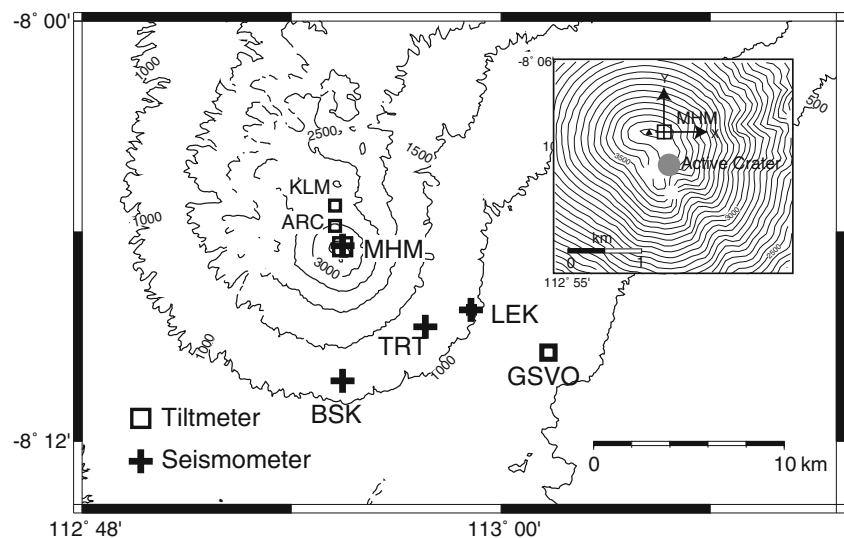
(h) Gas burst (Mar. 11, 2010)



were operated in 2007; however, most of the seismograms associated with Vulcanian eruptions were saturated because

of the narrow dynamic range of the frequency modulation, so we do not include these seismic data in the analysis.

**Fig. 2** Location map of tilt and seismic stations with topography of Mt. Semeru. *Y* and *X*-axes in the *insert* map represent the north–south and east–west components of the tilt meter

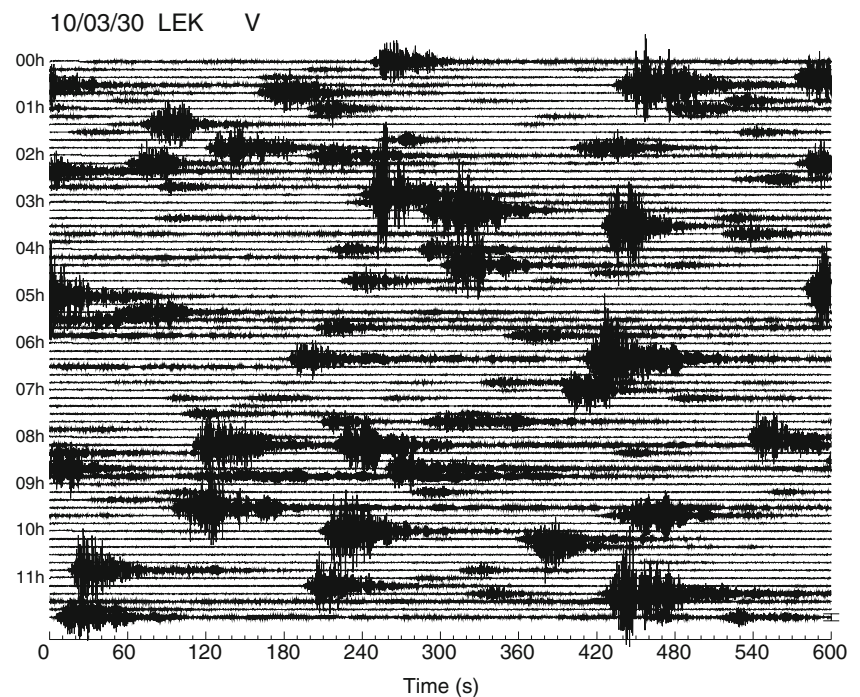


During both observation periods, Semeru Volcano repeatedly exploded at intervals of a few minutes to tens of minutes, with each explosion exciting seismic waves. Figure 3 shows an example of seismic data recorded in 2010. Signals with large amplitudes and durations of about 60 s are records of volcanic eruptions (called explosion earthquakes; hereafter, EXs). In spite of the short observation period (about 3–4 weeks), we recorded more than 1,000 eruptions, which is an adequate dataset to capture the basic characteristics of the two styles of eruptions.

### Inflation prior to Vulcanian eruptions in 2007

Figure 4 shows records of the seismic and tilt signals associated with a Vulcanian eruption. Although microseismic oceanic noise with periods of approximately 2–10 s is large, we observe a gradual uplift tilt in the direction of the active crater before each eruption. To reduce the effect of unknown long-period noise and long-term drift in the tilt signals, we stack the tilt signals from many eruptions. We select Vulcanian eruptions that had occurred after repose periods longer than 10 min and that had ambient tilt noise <15 nrad. To

**Fig. 3** Seismic records from LEK station for steam bursts in March 2010





07/04/09/ 08h44m40s

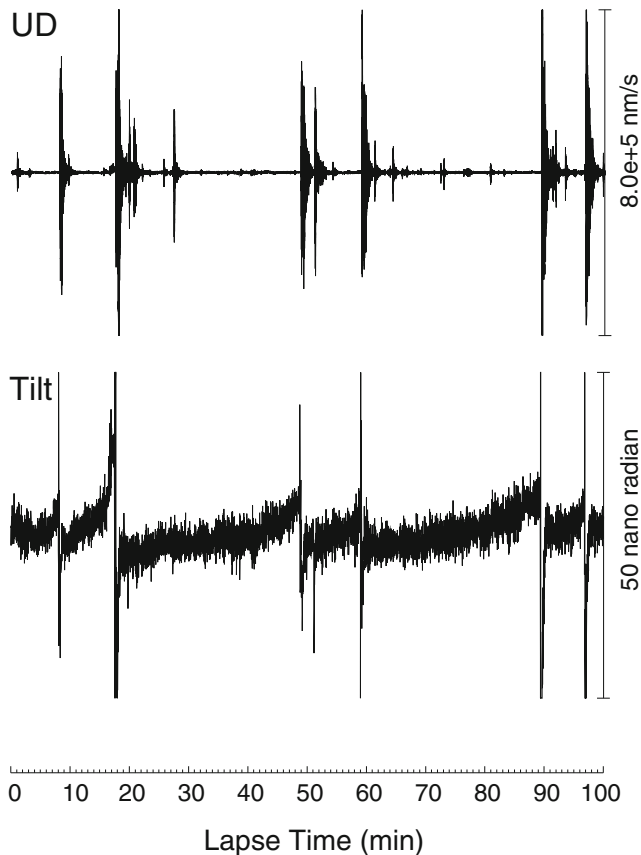


**Fig. 4** Examples of tilt records and seismic signals associated with Vulcanian eruptions in 2007. The *top trace* is the vertical component of the broadband seismometer at MHM. The *bottom trace* shows the radial component of tilt in which the upward direction indicates uplift toward the active crater

reduce the noise resulting from diurnal temperature variations and other unknown long-period noise, we detrend the tilt signals by fitting the data to a time-dependent linear function over the interval of 600 to 420 s before each eruption. We then stack the data with adjustment to set the onset time of each eruption as the time at which the initial phase of the explosion earthquake is recorded at MHM. This is adequate since the time differences between the seismic phase and eruption time estimated from infrasonic records is generally less than a few seconds (Iguchi et al. 2008).

Figure 5 shows the stacked tilt records for more than 400 events (see top trace of “ALL”). Inflation starts from 200 to 300 s prior to each Vulcanian eruption and seems to accelerate at 30–40 s before the eruption.

The amplitude of EXs is related to the pressure inside the conduit and/or the size of conduit before the eruption (e.g., Kanamori et al. 1984; Nishimura and Hamaguchi 1993). To examine the magma ascent and pressurization processes in the conduit, we compare the tilt signals prior to Vulcanian

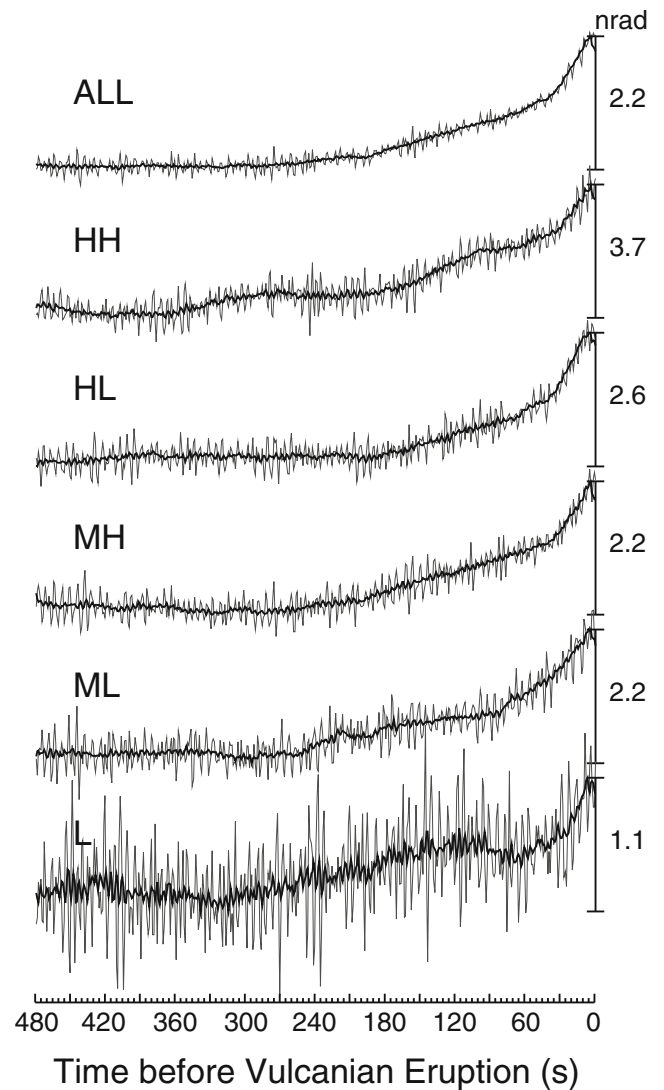


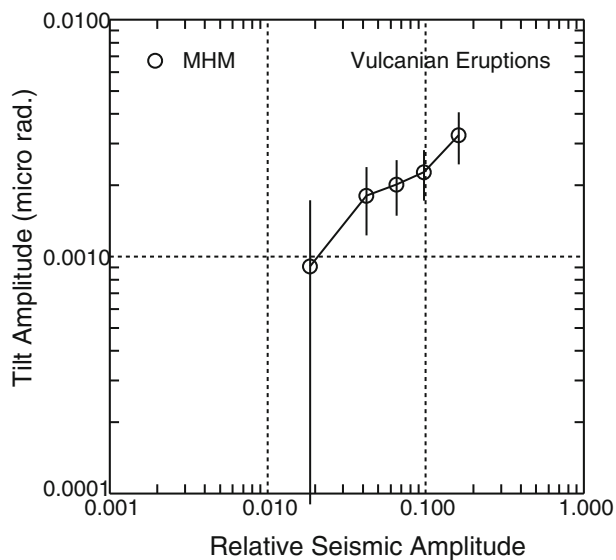
**Fig. 5** Stacked tilt records for Vulcanian eruptions. Each *thin line* represents stacked tilt records for events with different magnitudes of EXs. The *top trace* marked “ALL” is a stack including all the explosions satisfying the criteria (see text for details). *HH, HL, MH, ML, and L* are stacked tilt signals for different magnitudes of EXs. *Thick lines* represent the tilt records averaged over 6 s

eruptions with distinct maximum amplitudes of EXs at MHM. We categorize the eruptions into five groups, classified into evenly spaced amplitudes on a logarithmic scale. We use the notations of HH, HL, MH, ML, and L to represent different amplitudes of EXs ranging from large to low. The stacked tilt records are shown separately for each group in Fig. 5. The tilt signals normalized by the amount of tilt change during inflation in each trace show a similar pattern of temporal changes in each of the five groups: inflation starts about 200–300 s prior to the Vulcanian eruption, and the inflation rate accelerates with time. In contrast to this trend, the amount of tilt related to the seismic amplitude of EXs shows an almost linear increase in tilt amplitude versus seismic amplitude on a logarithmic scale (Fig. 6).

### Inflation prior to gas bursts in 2010

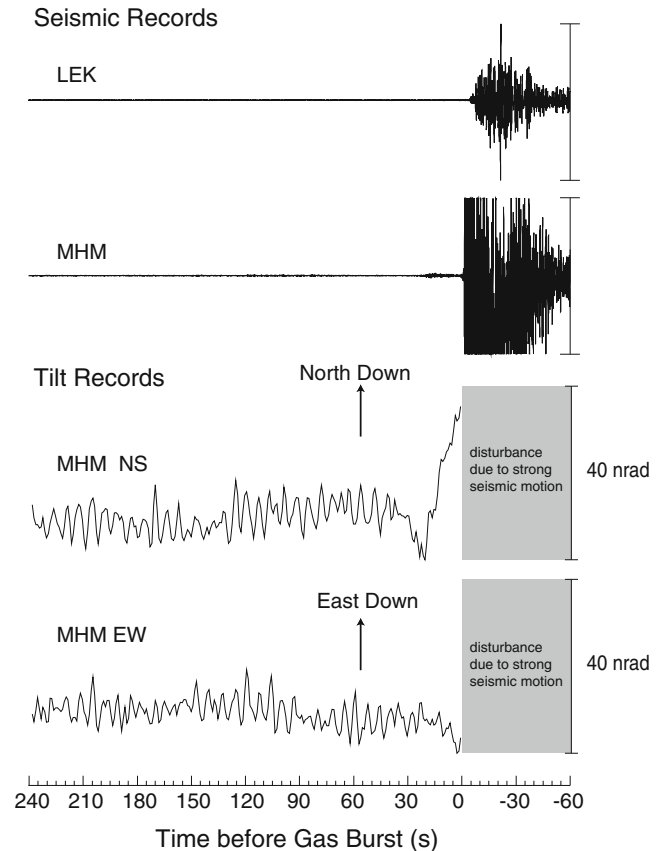
Figure 7 shows an example of the seismic and tilt signals that are associated with a gas burst. The tilt signal records show that inflation starts about 20 s before the gas burst. The amplitude of the NS component is much larger than that of the EW component, which suggests a pressure source at or below the active crater. Since microseismic oceanic noise is large, we apply the same procedure as explained above to obtain the basic characteristics of inflation tilt prior to gas bursts. We stack more than 500 tilt signals having a noise amplitude of  $<25$  nrad for each of the five groups separated according to the amplitudes of the EXs. Since the seismic signals at the nearest station, MHM, were saturated, we used the EXs recorded at distant stations LEK, BSK, and TRT. We analyzed the signals recorded on the NS component which is nearly radial to the active crater. Differences in the threshold levels of noise amplitudes (25 nrad for gas burst data and 15 nrad for Vulcanian eruption data) are due to differences in observation periods and recording systems.

Figure 8 shows a comparison of the tilt signals stacked according to the seismic amplitudes recorded at LEK. The tilt records, normalized by the amount of tilt change until the occurrence of eruptions, are quite similar to each other. The inflation starts consistently at 20 s prior to the gas burst, independent of the seismic amplitude accompanying the gas burst, and the tilt increases at a constant rate in each trace. Inflation for the lowest amplitude signals (L) starts a little earlier (30 s before the gas burst), indicating a small difference in the duration of inflation. However, due to minor ambiguity in reading the onset times of EXs with small amplitudes, we



**Fig. 6** Relation between tilt and seismic amplitude at MHM for Vulcanian eruptions. Vertical lines represent errors determined from noise amplitudes of stacked tilt signals. Seismic amplitude is normalized by  $1 \times 10^7$  nm/s

2010/03/27 01h33m



**Fig. 7** Examples of tilt records and seismic signals associated with a gas burst. The top two traces are vertical components of the short-period seismometer at MHM and LEK. The bottom two traces represent the NS and EW components of tilt meter. The NS component is nearly radial to the active crater

do not discuss this point further in the present study. The tilt amplitude increases with seismic amplitude at the three flank stations (Fig. 9), indicating that the magnitude of EXs is controlled by the amplitude of inflation or the inflation rate.

### Discussion

We have clarified common features and differences in volcanic inflation signals observed prior to Vulcanian eruptions and gas bursts at Semeru volcano. For both types of eruptions, the magnitude of EXs, which is one of the indicators of the strength of the eruption, increased with increasing tilt amplitude. As the precursor signals of inflations are automatically detected and used to predict the occurrence time of volcanic eruptions at Semeru Volcano (Hery et al. 2008), the relationship between tilt and seismic amplitudes enables us to predict the magnitude of eruptions based on geodetic data recorded close to the active crater. However, in order to take advantage

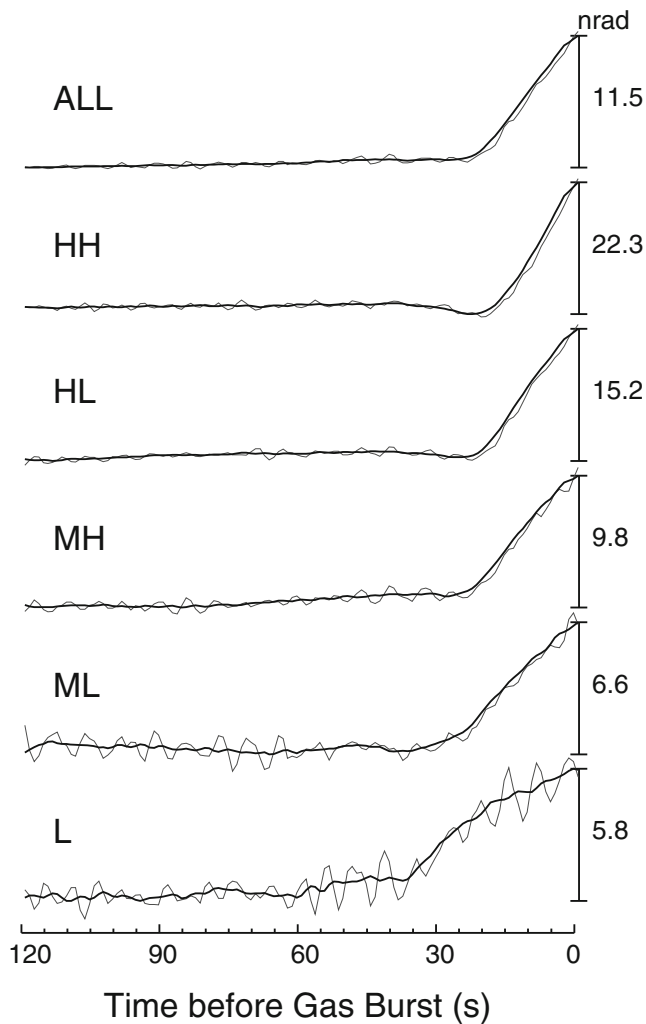


**Fig. 8** Stacked tilt records for gas explosions. The same as in Fig. 5

of this relationship, efforts must be made to mitigate the effect of noise in the raw data.

We also found significant differences in temporal changes of the inflation: Vulcanian eruptions followed accelerated changes in tilt occurring about 200–300 s prior to eruption, whereas gas bursts are preceded by inflation about 20 s prior to eruption without significant tilt acceleration. Accelerating tilt prior to eruption has been observed at other volcanoes. For example, at Stromboli Volcano, Italy, tilt prior to each explosion accelerated in proportion to the 1.5 power of time (Genco and Ripepe 2010). Temporal changes in the observed displacements prior to small Vulcanian eruptions at Suwanosejima, Japan, also show accelerated changes (see Fig. 4 in Iguchi et al. 2008). In contrast to the literature available for magmatic eruptions, to the best of our knowledge, there are few reports that discuss the temporal changes in volcano inflation prior to gas eruptions.

Determination of the depth of the pressure source causing inflation is important in order to understand the physical processes that produce the different acceleration patterns. At Semeru Volcano in 2009, we made tilt observations at stations

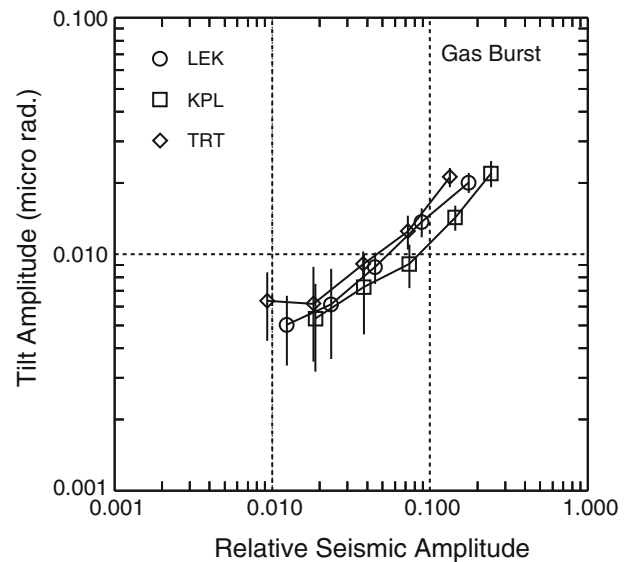


**Fig. 9** Relation of tilt and seismic amplitudes for gas bursts. Circles, squares, and diamonds represent the maximum seismic amplitudes of EXs recorded at LEK, KPL, and TRT, respectively. Vertical lines represent errors determined from noise amplitudes of stacked tilt signals. Seismic amplitude is normalized by  $3 \times 10^5$  nm/s

ARC and KLM (Fig. 2) located 1.7 and 3 km north, respectively, of the active crater. The same type of tilt meters (Pinnacle, Co. Ltd.) as were used at MHM were installed at a depth of 4 m at each station. No significant change in tilt was recorded at ARC or KLM prior to the gas bursts, although the periods of successful measurements at these stations were not the same as for MHM. This suggests that the depth of the pressure source for the gas bursts is shallow, probably <1 km. At Suwanosejima Volcano in Japan, the pressure source depth is estimated to be 100 m beneath the crater based on the spatial distribution of volcano deformation (Iguchi et al. 2004). The tilt signals at Stromboli Volcano show an almost identical pattern of temporal changes at stations about 400–1,000 m (see Fig. 4 in Genco and Ripepe 2010). If inflation is caused by magma ascent at a shallow depth immediately before eruption, this implies that the pressure source depth was shallower than 400 m. This is because only stations closer to the source would be affected by depth change of the source, while more distant stations would not be affected. Comparison of the results at Semeru Volcano with those obtained at other volcanoes that exhibit repetitive explosions with magnitudes comparable to those of Semeru Volcano suggests that the source depths of eruptions at Semeru Volcano were likely less than a few hundred meters so that tilt signals were not affected by temporal changes in the source depth. Likewise, the observed acceleration of inflation observed at Semeru Volcano can be attributed mainly to temporal changes in the pressure source strength rather than to a change in depth of the pressure source.

Accelerated increase in tilt can be explained by an increase in the volume of gas phases in the magma, which expand and

lift the magma level upward. Nishimura (2009) presented two processes that can accelerate ground deformation: diffusive gas bubble growth and rising gas bubbles in magma. When gas bubble growth is mainly driven by the diffusion of water molecules in the melt, ground deformation is proportional to the 1.5 power of time in the far field. For gas bubbles rising in the melt due to buoyancy, accelerated changes of inflation are expected to occur because of the expansion of gas bubbles caused by a decrease in ambient pressure. However, for magma with a viscosity of  $10^3$ – $10^4$  Pa s and an initial gas bubble radius of 0.1 m at a depth of 10 m, about 25–250 min is necessary for the rising gas bubbles to reach the ground surface. This is very long compared to the observed period of accelerated inflation (200–300 s), so gas bubble rise is unlikely to be a cause of inflation. Volcanic gases can rise through fractured and broken melt in the viscous melt (Goto 1999; Gonnermann and Manga 2003; Tuffen et al. 2003; Okumura et al. 2010). If the path along the fractures to the ground surface is not completely open and the gases expand the total volume of magma in the conduit, accelerated change is expected to be observed in ground deformation.

Our observations show a constant duration of inflation, independent of the amplitude of the EXs, which suggests an absence of temporal change in magma properties during the eruptive activity. In the case that diffusive gas bubble growth in magma is the dominant process for the inflation, the constant duration implies that the concentration and diffusivity of volatiles in the melt and the number density of gas bubbles do not change during the observation as much as suggested by gas bubble growth models (e.g., Prousevitch et al. 1993; Lyakhovsky et al. 1996; Shimomura et al. 2006; Chouet et al. 2006). To achieve gas flow in fractured magma, a constant supply of gas from a greater depth is necessary, although the relationship between gas flow in fractured magma and ground deformation is not yet well investigated.

Our observations indicate that the amplitude of tilt change during inflations and seismic amplitudes of EXs are well correlated. This implies that the overpressure and/or size of the source (i.e., volume of the magma or cross-sectional area of the vent) change with the scale of Vulcanian eruptions.

We note that Vulcanian eruptions in 2005 and 2006 at Semeru volcano showed different inflation characteristics, although accelerated changes were also observed (see Fig. 7 in Nishi et al. 2007 and Fig. 5 in Iguchi et al. 2008). The tilt amplitudes in 2005 and 2006 are much larger ( $>0.1$   $\mu$ rad) than the tilt amplitude (0.01  $\mu$ rad) in 2007. Sawtooth-shaped tilt records were observed in the data from 2005 and 2006, indicating that volcano inflation started just after the end of the previous eruption. These differences are probably related to the differences in magma properties and magma supply from deeper regions.

For gas bursts at Semeru Volcano, it may be reasonable to assume a constant supply of gas from a deeper region to

shallow depths in order to generate multiple explosions. However, a mechanism that can explain the observed constant rate of inflation and magnitude-dependent inflation as well as the timescale of 20 s is unknown. These factors should be considered in the development of a physical model of magmatic eruptions and gas bursts.

## Summary

We examined the characteristic behaviors of inflations prior to Vulcanian eruptions and gas bursts at Semeru Volcano based on analyses of tilt data and seismic records. The two styles of volcanic eruptions are preceded by inflations characterized by distinct temporal properties. Inflation starts about 20 s before each gas burst and proceeds at a constant rate, whereas Vulcanian eruption follows an accelerating inflation that starts 200–300 s before the explosion. The seismic amplitudes of the earthquakes associated with these eruptions increase with inflation, suggesting that we may be able to predict the magnitude of eruptions based on geodetic measurements.

**Acknowledgments** This study was supported in part through the SATREPS project “Multi-disciplinary Hazard Reduction from Earthquakes and Volcanoes in Indonesia” in collaboration with JST, JICA, RISTEK, and LIPI. Careful reviews by Drs. Michael Manga, Bernard Chouet, and Oleg Melnik improved the manuscript. Tilt and seismic observations were funded in part by Grants-in-Aid for Scientific Research (no. 14080205 and no. 20310104) from the Japanese Ministry of Education, Culture, Sports, Science, and Technology.

## References

- Chouet B, Dawson P, Nakano M (2006) Dynamics of diffusive bubble growth and pressure recovery in a bubbly rhyolitic melt embedded in an elastic solid. *J Geophys Res* 111:B07310. doi:10.1029/2005JB004174
- Genco R, Ripepe M (2010) Inflation–deflation cycles revealed by tilt and seismic records at Stromboli Volcano. *Geophys Res Lett* 37: L12302. doi:10.1029/2010GL042925
- Gonnermann HM, Manga M (2003) Explosive volcanism may not be an inevitable consequence of magma fragmentation. *Nature* 426:432–435
- Goto A (1999) A new model for volcanic earthquake at Unzen Volcano: melt rupture model. *Geophys Res Lett* 26:2541–2544
- Hery K, Iguchi M, Hendrasto M (2008) Automatic and real-time processing of tilt records for prediction of explosions at Semeru Volcano, East Java, Indonesia. *Indonesian J Phys* 19:69–74
- Iguchi M, Tameguri T, Mori T, Takayama T, Yakiwara H, Hirano S, Ohkura T, Yoshikawa S (2004) Very long-period seismic pulse associated with small-scale eruptions at Suwanosejima Volcano, Ryukyu Islands, Japan. In: Ida Y (ed) Report of Grants-in-Aid for Scientific Research in 2003 “Dynamics of Volcanic Explosion”, pp 61–66 (in Japanese)
- Iguchi M, Yakiwara H, Tameguri T, Hendrasto H, Hirabayashi J (2008) Mechanism of explosive eruption revealed by geophysical observations at the Sakurajima, Suwanosejima and Semeru volcanoes. *J Volcanol Geotherm Res* 178:1–9



- Kanamori H, Given JW, Lay T (1984) Analysis of seismic body waves excited by the Mt. St. Helens eruption of May 18. *J Geophys Res* 89:1856–1866
- Linde AT, Sacks S, Hidayat D, Voight B, Clarke A, Elsworth D, Mattioli G, Malin P, Shalev E, Sparks S, Widiwijayanti C (2009) Vulcanian explosion at Soufrière Hills Volcano, Montserrat on March 2004 as revealed by strain data. *Geophys Res Lett* 37: L00E07. doi:[10.1029/2009GL041988](https://doi.org/10.1029/2009GL041988)
- Lyakhovskiy V, Hurwitz S, Navon O (1996) Bubble growth in rhyolitic melts: experimental and numerical investigation. *Bull Volcanol* 58:19–32
- Melnik O, Sparks RSJ (1999) Nonlinear dynamics of lava dome extrusion. *Nature* 402:37–41
- Nishi K, Hendrasto M, Rosadi U, Purbawinata MA (2007) Micro-tilt changes preceding summit explosions at Semeru Volcano, Indonesia. *Earth Planets Space* 59:151–156
- Nishimura T (2009) Ground deformation caused by magma ascent in an open conduit. *J Volcanol Geotherm Res* 187(3–4):178–192. doi:[10.1016/j.jvolgeores.2009.09.001](https://doi.org/10.1016/j.jvolgeores.2009.09.001)
- Nishimura T, Hamaguchi H (1993) Scaling law of volcanic explosion earthquake. *Geophys Res Lett* 20:2479–2482
- Nishimura T, Ueki S (2011) Seismicity and magma supply rate of the 1998 failed eruption at Iwate Volcano. *Japan Bull Volcanol* 73:133–142
- Okumura S, Nakamura M, Nakano T, Uesugi K, Tsuchiyama A (2010) Shear deformation experiments on vesicular rhyolite: implications for brittle fracturing, degassing, and compaction of magmas in volcanic conduits. *J Geophys Res* 115. doi:[org/10.1029/2009JB006904](https://doi.org/10.1029/2009JB006904)
- Prousevitch AA, Sahagian DL, Anderson AT (1993) Dynamics of diffusive bubble growth in magmas: isothermal case. *J Geophys Res* 98:22283–22307
- Shimomura Y, Nishimura T, Sato H (2006) Bubble growth processes in magma surrounded by an elastic medium. *J Volcanol Geotherm Res* 155:307–322. doi:[10.1016/j.jvolgeores.2006.04.003](https://doi.org/10.1016/j.jvolgeores.2006.04.003)
- Tuffen H, Dingwell DB, Pinkerton H (2003) Repeated fracture and healing of silicic magma generate flow banding and earthquakes? *Geology* 31:1089–1092
- Voight B, Sparks RSJ, Miller AD, Stewart RC, Hoblitt RP et al (1999) Magma flow instability and cyclic activity at Soufriere Hills Volcano, Montserrat, British West Indies. *Science* 283:1138–1141
- Wylie JJ, Voight B, Whitehead JA (1999) Instability of magma flow from volatile-dependent viscosity. *Science* 285:1883–1885